AIP Journal of Applied Physics

The effect of the MgO buffer layer thickness on magnetic anisotropy in MgO/Fe/Cr/MgO buffer/MgO(001)

Anna Kozioł-Rachwał, Takayuki Nozaki, Vadym Zayets, Hitoshi Kubota, Akio Fukushima, Shinji Yuasa, and Yoshishige Suzuki

Citation: Journal of Applied Physics **120**, 085303 (2016); doi: 10.1063/1.4961203
View online: http://dx.doi.org/10.1063/1.4961203
View Table of Contents: http://scitation.aip.org/content/aip/journal/jap/120/8?ver=pdfcov
Published by the AIP Publishing

The effect of the MgO buffer layer thickness on magnetic anisotropy in MgO/Fe/Cr/MgO buffer/MgO(001)

Anna Kozioł-Rachwał,[1,2,a)] Takayuki Nozaki,[1] Vadym Zayets,[1] Hitoshi Kubota,[1] Akio Fukushima,[1] Shinji Yuasa,[1] and Yoshishige Suzuki[1,3]
[1]*National Institute of Advanced Industrial Science and Technology, Spintronics Research Center, Tsukuba, Ibaraki 305-8568, Japan*
[2]*AGH University of Science and Technology, Faculty of Physics and Applied Computer Science, al. Mickiewicza 30, 30-059 Kraków, Poland*
[3]*Graduate School of Engineering Science, Osaka University, 1-3 Machikaneyama, Toyonaka, Osaka 560-8531, Japan*

(Received 21 June 2016; accepted 4 August 2016; published online 23 August 2016)

The relationship between the magnetic properties and MgO buffer layer thickness d was studied in epitaxial MgO/Fe(t)/Cr/MgO(d) layers grown on MgO(001) substrate in which the Fe thickness t ranged from 0.4 nm to 1.1 nm. For $0.4\,\text{nm} \leq t \leq 0.7\,\text{nm}$, a non-monotonic coercivity dependence on the MgO buffer thickness was shown by perpendicular magneto-optic Kerr effect magnetometry. For thicker Fe films, an increase in the buffer layer thickness resulted in a spin reorientation transition from perpendicular to the in-plane magnetization direction. Possible origins of these unusual behaviors were discussed in terms of the suppression of carbon contamination at the Fe surface and changes in the magnetoelastic anisotropy in the system. These results illustrate a method to control magnetic anisotropy in MgO/Fe/Cr/MgO(d) via an appropriate choice of MgO buffer layer thickness d. *Published by AIP Publishing.* [http://dx.doi.org/10.1063/1.4961203]

INTRODUCTION

Perpendicular magnetic anisotropy (PMA) is a desirable property of ferromagnetic nanostructures, which has potential applications for high density magnetic random access memory (MRAM).[1–3] For the metal/oxide interfaces, PMA was reported in CoFe/CrO(AlO) (Ref. 4) and Co/oxide[5] structures, as well as in the CoFe(B)/MgO interface that enabled the realization of magnetic tunnel junction (MTJ) devices with perpendicularly magnetized CoFeB electrodes.[6–10] More recently, perpendicular magnetic order was observed in MgO/Fe/MgO,[11–13] Cr/Fe/MgO,[14–16] and V/Fe/MgO[15] structures. In the case of the Cr(V)/Fe/MgO system, the origin of the PMA was attributed to the anisotropy of the Fe/MgO interface; however, in the case of MgO/Fe/MgO, it was shown that both magneto-elastic and interface anisotropies are responsible for perpendicular magnetization alignment. First principles calculations performed by Shimabukuro *et al.* indicated that the perpendicular magnetic order at the Fe/MgO interface is a consequence of hybridization between the Fe 3d and the O 2p orbitals.[17] Nevertheless, recently, Hallal *et al.* have postulated that the origin of PMA in Fe/MgO is much more complex; they showed that the PMA energy propagates into the bulk Fe layers, showing a damped oscillatory character as a function of the Fe thickness.[18] Theoretical studies also predicted that magnetic anisotropy in Fe/MgO can be modified by an applied voltage,[19–21] which was confirmed by experimental studies for Au/Fe(Co)/MgO,[22–24] V/Fe/MgO,[25] and Cr/Fe/MgO.[26] Voltage control of magnetic anisotropy (VCMA) was demonstrated in the latter system for the Fe thicknesses $t = (0.3\text{–}0.7)$ nm. The amplitude of the VCMA effect as high as 300 fJ/Vm has been obtained for an Fe layer thickness of 0.45 nm, which is equivalent to 3 monolayers of Fe on MgO(001). High value of interface anisotropy and associated large voltage-induced changes are preferable for novel voltage-driven spintronic devices. Thus, a precise control of the magnetic properties and the ability to tune them are crucial. While magnetic anisotropy of ultrathin layers is sensitive to atomic-scale order at the interface, it can be significantly modified by strain, chemical intermixing, or surface morphology.

In this study, we investigated the influence of MgO seed layer thickness on the perpendicular magnetic anisotropy of ultrathin Fe films in MgO/Fe(t)/Cr/MgO(d)/MgO (001) structures. The evolution of magneto-optical Kerr effect (MOKE) hysteresis loops was studied for different MgO buffer layer thicknesses d. For the Fe thicknesses $t \leq 0.7$ nm, we observed a non-monotonic change in coercivity when the thickness of the MgO buffer was changed from 0 nm to 4 nm. For $0.8\,\text{nm} \leq t \leq 1.0\,\text{nm}$, the easy magnetization axis switched from out-of-plane to the in-plane orientation when the MgO buffer layer thickness was increased. Possible origins of these unusual behaviors were discussed in terms of carbon segregation at the Fe/Cr interface and changes in the magnetoelastic anisotropy in the system.

EXPERIMENTAL

The samples were grown in an ultrahigh vacuum (UHV) chamber. All the layers were deposited using an electron beam bombardment technique. The deposition rate was controlled by a quartz crystal monitor during the growth of the layers. A schematic drawing of the sample is shown in Figure 1. A double-side polished MgO(001) crystal was used as a substrate. The substrate was degassed under UHV by

[a)]a.koziolrachwal@aist.go.jp

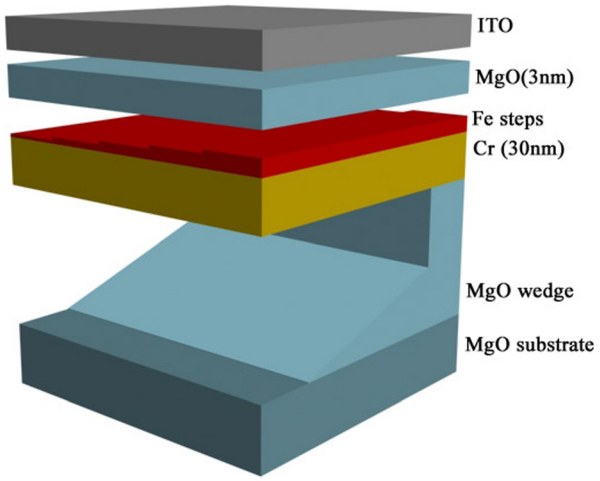

FIG. 1. Schematic drawing of the sample.

annealing at 800 °C for 10 min. A wedge-shaped homoepitaxial MgO(001) buffer layer was deposited at 200 °C for thicknesses (d) ranging from 0 nm to 4 nm over 16 mm. For some samples, a wedge with a thickness range (0–6) nm was used. After the deposition of the wedge, the evaporation of MgO was continued, which resulted in the formation of an MgO layer with a constant thickness of 15 nm. Following the MgO buffer layer deposition, a 30 nm-thick Cr layer was evaporated at 200 °C and annealed at 800 °C for 10 min. Next, Fe steps with thicknesses t varying between 0.4 nm and 1.1 nm were prepared on the Cr layer at a substrate temperature of 200 °C and annealed at 260 °C. After cooling the substrate to 60 °C, a 3 nm-thick MgO layer was deposited and annealed at 350 °C for 20 min. Finally, the sample was capped with a protective 20 nm-thick indium titanium oxide (ITO) layer deposited by sputtering. The ITO layer acts as a transparent capping layer for MOKE measurement. Figure 2 shows the reflection high-energy electron diffraction

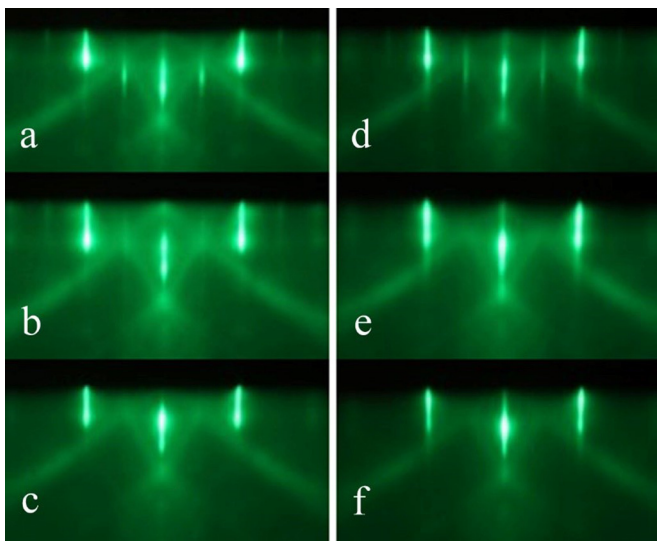

FIG. 2. RHEED patterns for the surface of a Cr buffer layer after annealing (a)–(c) and an Fe layer at t = 0.7 nm (d)–(f) collected for the sample regions with the MgO buffer layer thicknesses of 0 nm ((a) and (d)), 3 nm ((b) and (e)), and 15 nm ((c) and (f)). The incident electron beam is along Cr[110] and Fe[110] azimuths.

(RHEED) patterns from the Cr surface after annealing (a)–(c) and from an Fe layer with a thickness of 0.7 nm (d)–(f) after annealing at 260 °C. The patterns were collected from the sample regions without an MgO buffer layer ((a) and (d)), and with MgO buffer layers with thicknesses of $d = 3$ nm ((b) and (e)) and $d = 15$ nm ((c) and (f)). The incident electron beam was parallel to the MgO[100] azimuth. The pattern collected for the unbuffered Cr layer reveals half order streaks along MgO[100] (Figure 2(a)). The half-order streaks are still visible, but their intensities are diminished when the 3 nm MgO buffer layer was used (Figure 2(b)). For the Cr layer grown on the 15 nm-thick MgO buffer layer, a clean surface (1 × 1) pattern was registered, and thus, no reconstruction was observed (Figure 2(c)). After the deposition of the ultrathin Fe layer, an additional reconstruction appeared, but only for the unbuffered sample (Figure 2(d)). When an MgO layer was deposited on the Fe, the differences in the RHEED patterns vanished (not shown).

According to the previous experimental studies, both carbon and oxygen atoms can be responsible for c(2 × 2) reconstructions on Cr.[27] To elucidate the origin of the c(2 × 2) superstructure, Auger electron spectroscopy (AES) was used. Figure 3 (left) shows the AES spectra induced by 5 keV electrons collected at the Cr surface after annealing for different homoepitaxial buffer layer thicknesses. A carbon peak (267 eV) was found in all the measured spectra. Furthermore, an abrupt decrease in the C peak intensity with respect to the Cr signal (523 eV) was observed when the MgO thickness was increased from 2 nm to 5 nm (Figure 3, right). According to the previous experimental studies, sulfur and oxygen contaminations can also be responsible for c(2 × 2) reconstruction on Cr.[28] However, the AES spectrum collected for the lower kinetic energy for the Cr layer deposited directly on MgO(001) substrate showed no S contamination (not shown). The presence of oxygen peak could be detected as a shoulder of Cr $_{LMM}$ peak, and its presence is hard to judge. Nevertheless, we registered a decrease of the intensity of the half order streaks in RHEED pattern for the Cr layer with an increase of the MgO buffer layer thickness. If the additional reconstruction is related to the oxygen contamination at the Cr surface, it should not be sensitive to the change of the MgO buffer layer thickness. The results of the AES studies indicate that the surface reconstruction observed in RHEED could be attributed to the carbon impurities that segregate up from the MgO substrate during the growth and annealing of the Cr layer. Our observations confirm that a few nanometers-thick MgO buffer layer is an effective barrier against the diffusion of carbon into the Cr and Fe layers which is consistent with previous experimental studies.[29,30]

RESULTS AND DISCUSSION

The magnetic properties of the MgO/Fe/Cr/MgO layers were characterized by using MOKE measurements. Figure 4 shows representative perpendicular MOKE (PMOKE) hysteresis loops that were measured at room temperature for MgO/Fe/Cr layers grown on MgO buffer layers of different thicknesses, d. For the 0.4 nm Fe layer, we observed a non-hysteretic s-shaped loop at room temperature when the layer

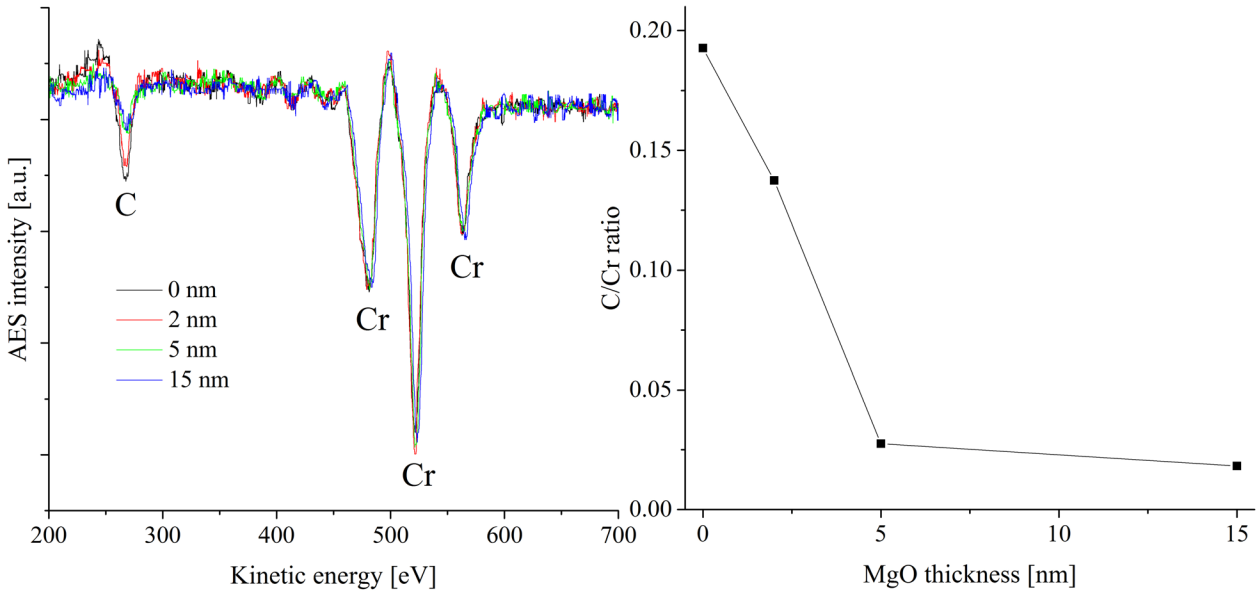

FIG. 3. Left: the AES spectra of Cr/MgObuffer(d)/MgO(001) collected for Cr layer grown on MgO buffer layer of varying thicknesses. All spectra are normalized to the Cr peak (at 521 eV). Right: Auger signal ratio (C at 267 eV/Cr at 521 eV) as a function of the MgO seed layer thickness.

was grown without an MgO buffer layer (Figure 4(a), black). Together with a decrease of temperature, a gradual decrease of saturation field and increase of remanence were noted in PMOKE (not shown), which reveals a superparamagnetic character of the loop measured at room temperature. When the buffer layer thickness was increased, a hysteretic behavior appeared; gradual increases in remanence and coercivity (H_c) were noted. Finally, for a 2 nm-thick MgO buffer layer, a loop with a full remanence and an out-of-plane coercivity of 1.3 kOe was observed (Figure 4(a), blue). A further increase of the buffer layer thickness resulted in a gradual decrease in coercivity from 1.3 kOe obtained for the 2 nm of MgO (Figure 4(a), blue) to 0.8 kOe registered for $d = 4$ nm (Figure 4(a), purple). For the Fe films in the (0.5–0.7) nm thickness range, clear influence of the MgO buffer layer thickness on coercivity was observed. Exemplary loops for an Fe thickness of 0.6 nm with different MgO buffer layer thicknesses are shown in Figure 4(b). The variation of H_c with respect to MgO buffer layer thickness d for Fe thicknesses of 0.5 nm, 0.6 nm, and 0.7 nm is summarized in Figure 5. For 0.5 nm $\leq t \leq$ 0.7 nm, a non-monotonic change in coercivity was noted as a function of d. The MgO thickness at which a maximum value of coercivity was obtained was shifted toward thinner MgO layers when the Fe thickness was increased from 0.5 nm to 0.7 nm. While a maximum H_c was registered at $d = 2.9$ nm for $t = 0.5$ nm, it was shifted to $d = 0.6$ nm for an Fe thickness of 0.7 nm with an H_c value of 1.4 kOe. Note that we did not observe change in the H_c for the Fe layers grown on MgO buffers with a thickness of 4 nm and 15 nm. The initial increase in coercivity can be understood in terms of a reduction of the carbon contamination at the Fe/MgO interface. Similar tendencies have been observed in the Fe/Au and Fe/Ag multilayer structures, where for the layers grown on carbon-free MgO substrates, enhanced values of surface anisotropy were noted in comparison with layers grown on carbon contaminated substrates.[31] Interestingly, thinner Fe layers require thicker MgO buffer layers to reach the maximum coercivity. This tendency indicates that in the sub-nanometer thickness regime, even small changes in Fe thickness (of about 1ML) affect the amount of carbon contamination at the Fe/MgO interface.

Although the origin of the initial enhancement in coercivity seems to be well understood, the decrease in H_c after attaining a maximum is an unexpected behavior. In the coherent rotation model, the coercivity is simply determined by the uniaxial magnetic anisotropy. However, in real systems, structural features, such as lattice defects, surface irregularities, or stress-driven structural changes result in changes in the shape of the hysteresis loop, especially its coercivity.[32] Therefore, we cannot unambiguously confirm whether the observed change in coercivity comes from the change in the effective anisotropy itself or not. Due to the limit of the amplitude of in-plane magnetic fields in our measurement system, we were not able to determine quantitative dependence between effective anisotropy and MgO buffer layer thickness for Fe layers thinner than 0.8 nm; however, the variation in effective anisotropy as a function of the MgO buffer layer thickness was quantitatively described for $t \geq 0.8$ nm. Figure 4(c) shows exemplary MOKE loops registered for a 1.0 nm-thick Fe layer as a function of d. The rectangular hysteresis loops with a low coercivity of 15 Oe were demonstrated in out-of-plane alignment at $d \leq 1$ nm (Figure 4(c), red). When the thickness of the MgO buffer layer was increased, a gradual decrease in remanence and an increase in the saturation field were noted in PMOKE, which indicated a spin reorientation transition (SRT) to the in-plane easy axis. For the 4 nm of MgO buffer layer, a rectangular hysteresis loop was registered in LMOKE (Figure 4(c), inset).

The MgO buffer layer thickness dependences of the estimated K_{eff} are summarized in Fig. 6 for $t = 0.9$ nm and $t = 1.0$ nm. For 3 nm $< d \leq$ 5.5 nm, the effective anisotropy constants were determined from the area between the

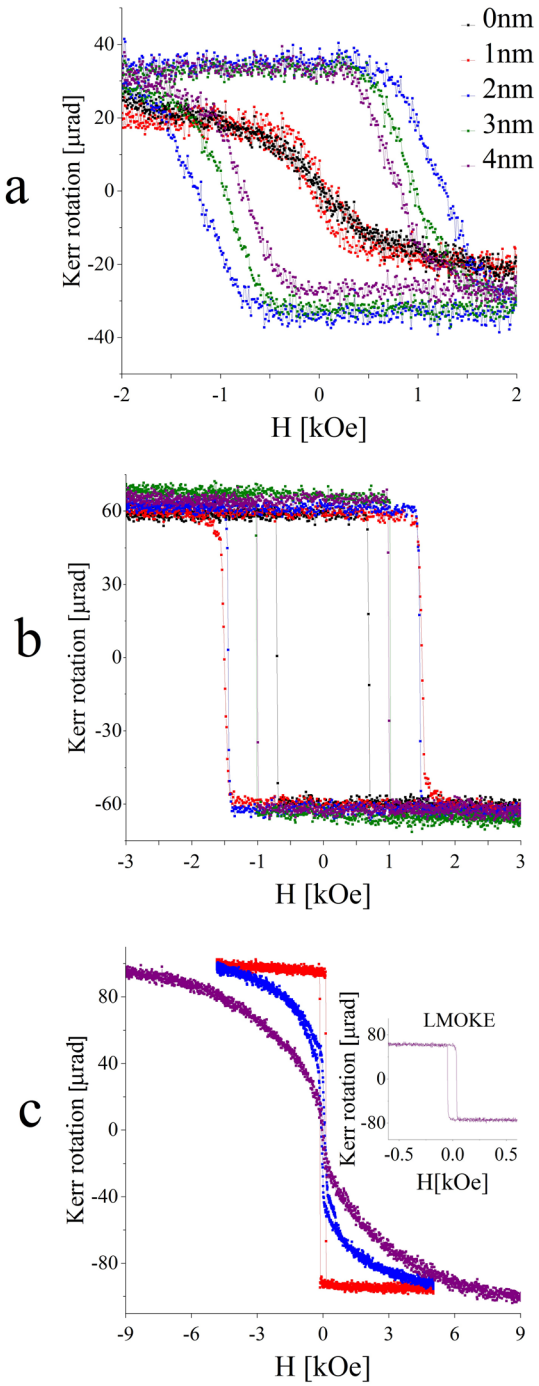

FIG. 4. PMOKE hysteresis loops measured for the Fe thickness of 0.4 nm (a), 0.6 nm (b), and 1.0 nm (c) in the MgO/Fe/Cr/MgO(d)/MgO(001) stack for different MgO seed layer thicknesses.

perpendicular and the in-plane magnetization loops in one of the hysteresis quadrants registered by MOKE. For an Fe thickness of 1.0 nm and an MgO thickness of 3 nm, the value of K_{eff} was determined from tunneling magnetoresistance (TMR) measurements in the Fe/MgO/Fe/Cr/MgO stack described in Ref. 24. In both methods, the value of the saturation magnetization, M_s, was evaluated by SQUID measurements. It should be noted that for a fixed Fe thickness we observed no significant change in the value of M_s for the Fe layers grown on buffer layers with different thicknesses within a 5% error (not shown here), indicating that the observed MgO thickness-driven SRT does not originate from the change in the shape anisotropy ($-2\pi M_s^2$), which favors in-plane magnetization alignment.

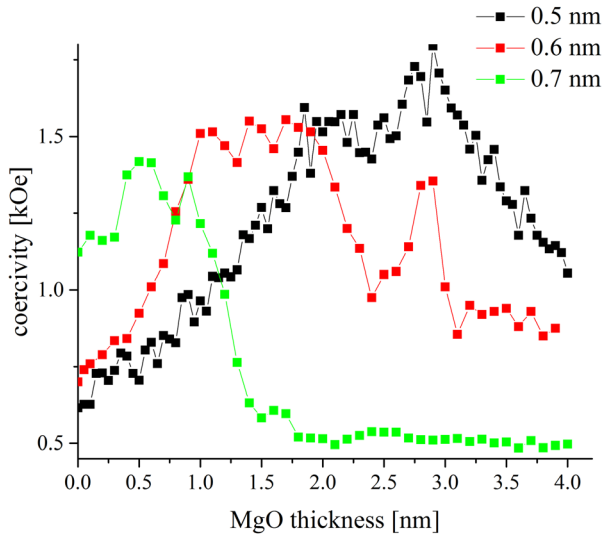

FIG. 5. Coercivity vs. MgO thickness dependence obtained for Fe thickness of 0.5 (black), 0.6 (red), and 0.7 nm (green). Lines are guides to the eye.

We observed clear reductions in the K_{eff} with increasing d and MgO-thickness-driven SRT. The critical thickness of MgO for which SRT occurred was reduced from (3.4 ± 0.2) nm to (1.3 ± 0.2) nm when the Fe thickness was increased from 0.9 nm to 1.0 nm. For thicker Fe layers, an in-plane direction of magnetization was noted over the whole MgO thickness range. The gradual decrease of K_{eff} with increasing buffer layer thickness indicates that its negative contribution to effective anisotropy is increased. Because we did not observe any distinct difference in the strength of the $K_{eff}(d)$ dependence between 0.9 nm and 1.0 nm, we expect that this negative contribution to K_{eff} has a volume origin rather than a surface origin.

The origin of the unexpected decrease in K_{eff} with increasing buffer layer thickness is ambiguous. One possible

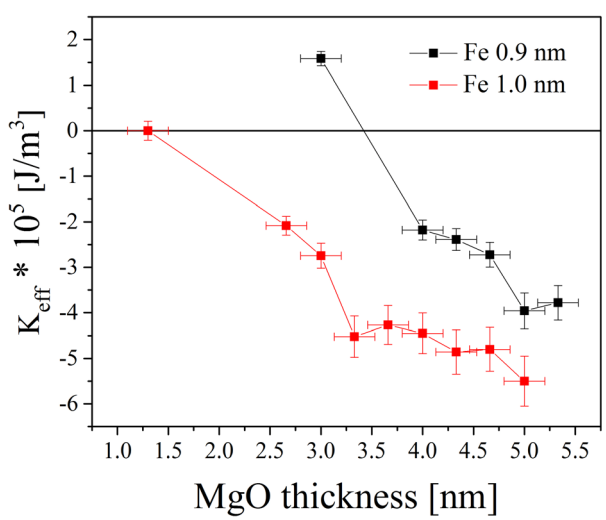

FIG. 6. K_{eff} as a function of MgO buffer layer thickness obtained for Fe thickness of 0.9 nm (black points) and 1.0 nm (red points). Line is guide to the eye.

explanation assumes a change in roughness in the Cr layer as a function of d. The interface roughness can give a contribution to magnetostatic energy and result in changes in perpendicular magnetic anisotropy.[33–37] However, in the case of our studies, for a given Fe thickness, we did not observe a notable change in M_s as a function of the MgO thickness, which suggests that the change in effective anisotropy is not induced by the modification of magnetostatic energy. This, together with the volume rather than surface origin of the effect, suggests that the change in effective anisotropy that we observed is induced by variation of magnetoelastic anisotropy contribution. At this point, two issues should be discussed. The first is the origin of the magnetoelastic anisotropy in MgO/Fe/Cr, and the second is the origin of the magnetoelastic anisotropy change with the variation in MgO buffer layer thickness d. The existence of the magnetoelastic anisotropy in MgO/Fe/Cr seems to be puzzling due to the small lattice misfit (around 0.6%) between Fe and Cr. However, the misfit can be enhanced if intermixing between Fe and Cr layers at the Fe/Cr interface is considered.[38] The presence of intermixing at the Fe/Cr interface has been suggested in previous studies.[39] To clarify this issue, the elemental composition of MgO/Fe/Cr/MgO with an Fe thickness of 1.5 nm and an MgO thickness of 3 nm was studied by electron energy loss spectroscopy (EELS). High-angle annular dark field scanning transmission electron microscopy (HAADF STEM) images and the EELS spectra were collected using the JEM–ARM200F microscope operating at 200 kV in the STEM mode. Figure 7 shows HAADF STEM image (left) and the EELS spectra collected as a function of distance from the Fe/Cr interface. The size of the probe was 0.5 nm. The spectrum captured from the sample region below the Fe/Cr interface (Figure 7, purple) shows both Cr $L_{2,3}$ and Fe $L_{2,3}$ edges, which are evidence that diffusion of Fe into the interface near Cr occurs. The spectra registered from the sample regions situated within the Fe layers beside the Fe $L_{2,3}$ edge reveal the existence of a Cr $L_{2,3}$ edge. The (Cr L_3)/(Fe L_3) intensity ratio was decreased with an increasing distance from the Fe/Cr interface, which indicates a decreasing degree of Fe-Cr intermixing as a function of the distance from the Fe/Cr interface. The Fe/Cr alloying should affect the magnetic properties of the system. For a reference sample with a MgO buffer layer thickness of $d_{MgO} = 3$ nm, a reduction in the saturation magnetization compared with the bulk value was noted for $t_{Fe} \leq 1.0$ nm;[26] M_s value of 1.65 T for $t_{Fe} = 0.4$ nm and $M_s = 1.95$ T for $t_{Fe} = 1.0$ nm were obtained at room temperature. Because for the Fe/MgO interface an enhancement of magnetic moment of Fe is expected,[40] a decrease of M_s value noted for a subnanometer Fe is rather related to the reduction of magnetic moment of Fe at Fe/Cr interface or intermixing between Fe and Cr.[41] Nevertheless, even for an Fe layer as thin as 0.4 nm for $d \geq 2$ nm, we observed a stable magnetic state at room temperature. Since the signal from Cr was noted even at 0.5 nm from the Fe/Cr interface in the EELS spectra (Figure 7, black), the role of Fe-Cr intermixing and its influence on perpendicular magnetic anisotropy in the MgO/Fe/Cr system should be considered in future studies. To conclude, the origin of magnetoelastic anisotropy in MgO/Fe/Cr can be related to the enhanced in-plane lattice constant of the Fe layer that is induced by Fe-Cr intermixing at the Fe/Cr interface. Although there have been no theoretical studies concerning the dependence of the perpendicular magnetic anisotropy on the in-plane lattice constant for the Fe/MgO system, first principles calculations made for FeCo/MgO layers showed that an increase in the in-plane lattice constant of FeCo results in an increase in the negative contribution to the effective anisotropy.[42] The existence of additional negative contribution to the magnetic anisotropy, besides shape and magnetocrystalline anisotropy, was confirmed for MgO/Fe/Cr layers grown on 3 nm-thick MgO buffer as a result of systematic studies of effective anisotropy dependence on Fe thickness (a method used to obtain K_{eff} was described in Ref. 26). Figure 8 shows $K_{eff}\, t$ plotted as a function of Fe thickness for $t > 0.6$ nm. The slope of the $K_{eff}\, t(t)$ dependence, which indicates volume anisotropy contribution,[43] was estimated to be -2.38×10^6 J/m^3. Such a value is much larger than the sum of the magnetocrystalline anisotropy (which is equal to -4.8×10^4 J/m^3 for bulk Fe) and the shape anisotropy (which is of the order of -1×10^6 J/m^3), which means

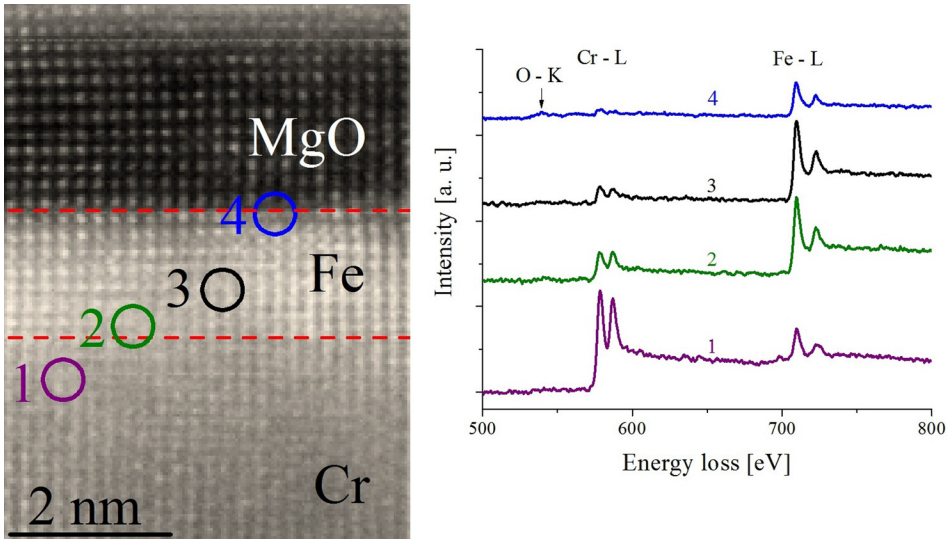

FIG. 7. Left: HAADF STEM image of the MgO/Fe(1.5 nm)/Cr sample used for EELS measurement. Red lines indicate the position of Cr/Fe and Fe/MgO interfaces. Right: EELS spectra (in the range of 500 eV–750 eV) integrated over the selected regions (1–4).

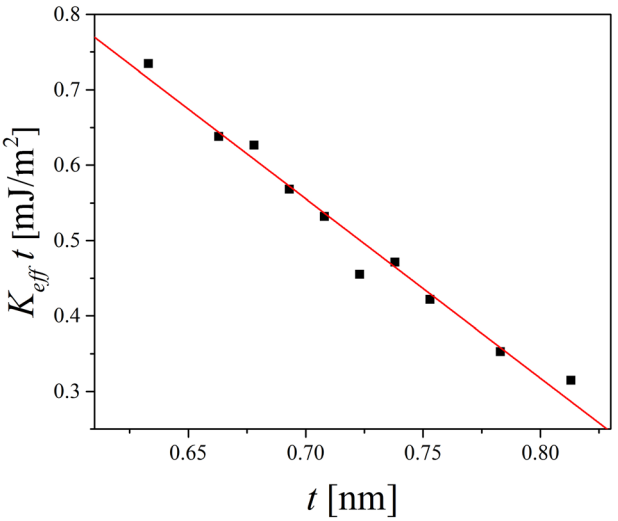

FIG. 8. K_{eff} t as a function of Fe thickness obtained for MgO/Fe(t)/Cr grown on 3 nm-thick MgO buffer layer. Slope indicates volume contribution to the effective anisotropy.

that an additional negative contribution is included. This negative contribution can be attributed to the magnetoelastic anisotropy. Finally, the variation in the magnetoelastic anisotropy contribution as a function of MgO buffer layer thickness should be discussed. The reduction of the magnetoelastic anisotropy contribution with an MgO buffer thickness can be explained if a change in the density of defects at the Cr surface is assumed. In our studies, we obtained an increase in the negative contribution to K_{eff} with increasing MgO buffer layer thickness, indicating that the change of defect density that is expected for different thicknesses of MgO layers is responsible for the variation of perpendicular magnetic anisotropy. This suggests that in the proximity of defects, a lattice relaxation occurs that results in a change of the positive contribution to K_{eff}.

For the Fe layers thinner than 0.8 nm, the change of MgO buffer layer thickness caused a modification of the coercivity in the hysteresis loops. As it was shown, the initial increase in coercivity is related to a decrease in carbon contamination at the Fe surface, which affects the surface anisotropy contribution. After gaining a critical MgO thickness, a gradual decrease in coercivity (or even the non-monotonic change in H_c vs. d for an Fe thickness of 0.6 nm) was noted. Although we were not able to determine the dependence of $K_{eff}(d)$ for films with $t < 0.8$ nm, according to the results obtained for thicker Fe layers, we can expect that a gradual decrease of coercivity above the critical MgO thickness registered in PMOKE loops is a result of change of magnetoelastic anisotropy, analogically to the results observed for $t \geq 0.8$ nm.

CONCLUSIONS

In summary, we showed that by changing the MgO buffer layer thickness in the MgO/Fe(t)/Cr/MgO(d) stack, the magnetic properties of the Fe layers can be tuned. For the thinnest Fe layers ($t = 0.4$ nm), increasing of the MgO thickness from 0 to 2 nm resulted in a transition from the superparamagnetic to the ordered magnetic state. Further increases in d influenced the coercivity of the hysteresis loops. For the Fe thicknesses in the range of (0.5–0.7) nm, a non-monotonic change of out-of-plane coercivity was noted with changing buffer layer thickness. Finally, for the Fe thicknesses of 0.9 nm and 1.0 nm, an MgO thickness-driven spin reorientation transition from out-of plane to in-plane was observed. There are at least two effects that are responsible for the behaviors we observed. The first is related to a reduction in carbon contamination at the Fe/MgO interface. This effect manifests itself via an increase in coercivity as a function of MgO thickness for a very thin Fe layers ($t < 0.8$ nm). The second effect that is responsible for decrease in the coercive field as a function of MgO buffer layer thickness for Fe layers thinner than 0.8 nm and MgO-thickness driven SRT for thicker films ($0.8\text{ nm} \leq t \leq 1.0\text{ nm}$) is related to the changes in magnetoelastic anisotropy in the system. We hope that these results will stimulate theoretical discussions concerning the influence of the contribution of magnetoelastic anisotropy on the perpendicular magnetic anisotropy in the MgO/Fe/Cr system.

ACKNOWLEDGMENTS

We thank E. Usuda for assistance with the experiments and M. Ślęzak for low temperature MOKE measurements. This work was partly supported by ImPACT Program of Council for Science, Technology Grants-in-Aid for Scientific Research (26709046).

[1]A. Brataas, A. D. Kent, and H. Ohno, Nat. Mater. **11**, 372–381 (2012).
[2]T. Kawahara, K. Ito, R. Takemura, and H. Ohno, Microelectron. Reliab. **52**, 613–627 (2012).
[3]H. Yoda *et al.*, Curr. Appl. Phys. **10**, e87 (2010).
[4]S. Monso, B. Rodmacq, S. Auffret, G. Casali, F. Fettar, B. Gilles, B. Dieny, and P. Boyer, Appl. Phys. Lett. **80**, 4157 (2002).
[5]L. E. Nistor, B. Rodmacq, S. Auffret, and B. Dieny, Appl. Phys. Lett. **94**, 012512 (2009).
[6]S. Ikeda, K. Miura, H. Yamamoto, K. Mizunuma, H. D. Gan, M. Endo, S. Kanai, J. Hayakawa, F. Matsukura, and H. Ohno, Nat. Mater. **9**, 721 (2010).
[7]A. D. Kent, Nat. Mater. **9**, 699–700 (2010).
[8]S. Yakata, H. Kubota, Y. Suzuki, K. Yakushiji, A. Fukushima, S. Yuasa, and K. Ando, J. Appl. Phys. **105**, 07D131 (2009).
[9]V. B. Naik, H. Meng, and R. Sbiaa, AIP Adv. **2**, 042182 (2012).
[10]H. Sato, E. C. I. Enobio, M. Yamanouchi, S. Ikeda, S. Fukami, S. Kanai, F. Matsukura, and H. Ohno, Appl. Phys. Lett. **105**, 062403 (2014).
[11]A. Kozioł-Rachwał, T. Giela, B. Matlak, K. Matlak, M. Ślęzak, T. Ślęzak, M. Zając, R. Rüffer, and J. Korecki, J. Appl. Phys. **113**, 214309 (2013).
[12]A. Kozioł-Rachwał, W. Skowroński, T. Ślęzak, D. Wilgocka-Ślęzak, J. Przewoznik, T. Stobiecki, Q. H. Qin, S. van Dijken, and J. Korecki, J. Appl. Phys. **114**, 224307 (2013).
[13]J. Okabayashi, J. W. Koo, H. Sukegawa, S. Mitani, Y. Takagi, and T. Yokoyama, Appl. Phys. Lett. **105**, 122408 (2014).
[14]J. W. Koo, S. Mitani, T. T. Sasaki, H. Sukegawa, Z. C. Wen, T. Ohkubo, T. Niizeki, K. Inomata, and K. Hono, Appl. Phys. Lett. **103**, 192401 (2013).
[15]C.-H. Lambert, A. Rajanikanth, T. Hauet, S. Mangin, E. E. Fullerton, and S. Andrieu, Appl. Phys. Lett. **102**, 122410 (2013).
[16]J. W. Koo, H. Sukegawa, S. Kasai, Z. C. Wen, and S. Mitani, J. Phys. D: Appl. Phys. **47**, 322001 (2014).
[17]R. Shimabukuro, K. Nakamura, T. Akiyama, and T. Ito, Physica E (Amsterdam) **42**, 1014 (2010).
[18]A. Hallal, H. X. Yang, B. Dieny, and M. Chshiev, Phys. Rev. B **88**, 184423 (2013).
[19]K. Nakamura, T. Akiyama, T. Ito, M. Weinert, and A. J. Freeman, J. Magn. **16**, 161 (2011).
[20]C.-G. Duan, J. P. Velev, R. F. Sabirianov, Z. Zhu, J. Chu, S. S. Jaswal, and E. Y. Tsymbal, Phys. Rev. Lett. **101**, 137201 (2008).
[21]M. Tsujikawa and T. Oda, Phys. Rev. Lett. **102**, 247203 (2009).

[22]T. Maruyama, Y. Shiota, T. Nozaki, K. Ohta, N. Toda, M. Mizuguchi, A. A. Tulapurkar, T. Shinjo, M. Shiraishi, S. Mizukami, Y. Ando, and Y. Suzuki, Nat. Nanotechnol. **4**, 158 (2009).
[23]Y. Shiota, T. Maruyama, T. Nozaki, T. Shinjo, M. Shiraishi, and Y. Suzuki, Appl. Phys. Express **2**, 063001 (2009).
[24]T. Nozaki, Y. Shiota, M. Shiraishi, T. Shinjo, and Y. Suzuki, Appl. Phys. Lett. **96**, 022506 (2010).
[25]A. Rajanikanth, T. Hauet, F. Montaigne, S. Mangin, and S. Andrieu, Appl. Phys. Lett. **103**, 062402 (2013).
[26]T. Nozaki, A. Kozioł-Rachwał, W. Skowroński, V. Zayets, Y. Shiota, S. Tamaru, H. Kubota, A. Fukushima, S. Yuasa, and Y. Suzuki, Phys. Rev. Appl. **5**, 044006 (2016).
[27]J. S. Foord, A. P. C. Reed, and R. M. Lambert, Surf. Sci. **129**, 79 (1983).
[28]J. Lagoute, S. L. Kawahara, C. Chacon, V. Repain, Y. Girard, and S. Rousset, J. Phys. Condens. Matter **23**, 045007 (2011).
[29]M. Sicot, S. Andrieu, C. Tiusan, F. Montaigne, and F. Bertran, J. Appl. Phys. **99**, 08D301 (2006).
[30]A. Kozioł-Rachwał, T. Ślęzak, M. Ślęzak, K. Matlak, E. Młyńczak, N. Spiridis, and J. Korecki, J. Appl. Phys. **115**, 104301 (2014).
[31]M. Rickart, B. F. P. Roos, T. Mewes, J. Jorzick, S. O. Demokritov, and B. Hillebrands, Surf. Sci. **495**, 68 (2001).
[32]A. Hubert and R. Schäfer, *Magnetic Domains* (Springer, 2009).
[33]E. Schlömann, J. Appl. Phys. **41**, 1617 (1970).
[34]P. Bruno, J. Phys. F: Met. Phys. **18**, 1291 (1988).
[35]P. Bruno, J. Appl. Phys. **64**, 3153 (1988).
[36]Y. P. Zhao, G. Palasantzas, G. C. Wang, and J. T. M. D. Hosson, Phys. Rev. B **60**, 1216 (1999).
[37]S. B. Choe and S. C. Shin, J. Magn. Magn. Mater. **221**, 255 (2000).
[38]V. Razumovskiy, A. V. Ruban, and P. A. Korzhavyi, Phys. Rev. B **84**, 024106 (2011).
[39]P. Sheng, F. Bonell, S. Miwa, T. Nakamura, Y. Shiota, S. Murakami, D. D. Lam, S. Yoshida, and Y. Suzuki, Appl. Phys. Lett. **102**, 032406 (2013).
[40]E. Jal, J. B. Kortright, T. Chase, T. M. Liu, A. X. Gray, P. Shafer, E. Arenholz, P. Xu, J. Jeong, M. G. Samant, S. S. P. Parkin, and H. A. Dürr, Appl. Phys. Lett. **107**, 092404 (2015).
[41]S. Mirbt, I. A. Abrikosov, B. Johansson, and H. L. Skriver, Phys. Rev. B **55**, 67 (1997).
[42]K. H. He and J. S. Chen, J. Appl. Phys. **111**, 07C109 (2012).
[43]U. Gradmann and J. Müller, Phys. Status Solidi **27**, 313 (1968).